Available online at www.sciencedirect.com
SCIENCE DIRECT
Catalysis Today 99 (2005) 143–149
CATALYSIS TODAY
www.elsevier.com/locate/cattod

Photocatalysed selective oxidation of cyclohexane to benzene on MoO_x/TiO_2

P. Ciambelli*, D. Sannino, V. Palma, V. Vaiano

Dipartimento di Ingegneria Chimica e Alimentare, Università di Salerno, 84084 Fisciano (SA), Italy

Available online 15 December 2004

Abstract

Heterogeneous oxidative dehydrogenation of cyclohexane to benzene was found to occur under photocatalytic conditions on MoO_x/TiO_2. Initial cyclohexane conversion of 15% and maximum selectivity to benzene of 65% were achieved at 308 K on 8 wt.% MoO_x/TiO_2 under irradiation with a continuous flow reactor. The main by-product was carbon dioxide. Catalyst deactivation was observed. Titania exhibited high activity of total oxidation to carbon dioxide but was not selective for conversion to benzene. Polymolybdate species seem to be responsible for changing the selectivity of titania, favouring the formation of benzene. Nevertheless, when supported on α- or γ-alumina they promote only the formation of carbon dioxide.

Keywords: Photocatalytic oxidation; Cyclohexane; Benzene; MoO_x/TiO_2

1. Introduction

Heterogeneous photocatalytic oxidation has been extensively studied for environmental applications such as detoxification processes. Total oxidation of organics at room temperature on TiO_2 either in water and in air has been reported [1,2]. A drawback of these processes is the formation of partial oxidation products, sometimes resulting in increased toxicity of the treated stream. However, by reversing the final goal of the photocatalytic oxidation process a question is asked: is it possible to enhance the selectivity to partially oxidised products so much that the process could be used for their production? Few studies have been conducted on photocatalysis as potential technology for synthesis of chemicals from hydrocarbon feedstocks. In the 1970s pioneer works reported photo-oxidation of alkanes and alcohols in heterogeneous gas–solid reactors [3–6]. Alkanes have been oxidised on anatase TiO_2 achieving 75% selectivity to acetone at 3% isobutane conversion, 30% selectivity to butanone from *n*-butane, but complete oxidation from 1-butene and 2-butene [3]. In more recent works, few studies employed gas–solid reactors. Ethane was found to be photocatalytically oxidised to acetaldehyde and formaldehyde on MoO_3/SiO_2 by optimising the experimental conditions for high selectivity [7]. Ethanol was selectively converted to acetaldehyde and formaldehyde on TiO_2 [8]. Muggli and Falconer showed that selectivity of ethanol photocatalytic oxidation is changed as effect of titania sites poisoning by adsorption of reactants [9]. This seems suggest a way to design a selective catalyst for photocatalytic oxidation.

The most studies of cyclohexane photocatalytic oxidation deal with slurry systems. Cyclohexanol, cyclohexanone, and polyoxygenates have been obtained on silica supported vanadia or polyoxytungstate catalysts [10–14]. On titania [15] cyclohexane photo-oxidation in dichlorometane leads to the formation of cyclohexene traces.

The studies of Frei on photocatalysed oxidation of hydrocarbons in zeolite cages indicate a potential way to achieve high selectivity in gas–solid systems. Very impressive results (100% selectivity to aldehydes and ketones from the corresponding alkanes, cycloalkanes, alkenes, aromatics) are reviewed [16]. It is proposed that cyclohexanone is obtained from cyclohexane through a light induced radical mechanism resulting in the selective

* Corresponding author. Tel.: +39 089 964151; fax: +39 089 964057.
E-mail address: pciambelli@unisa.it (P. Ciambelli).

0920-5861/$ – see front matter © 2004 Elsevier B.V. All rights reserved.
doi:10.1016/j.cattod.2004.09.034

formation of ketone due to a confinement effect inside the zeolite cage [17].

Gas–solid heterogeneous photocatalytic oxidation of cyclohexane and cyclohexene in humidified air was studied at 303 K on P-25 titania powder [18]. Deep oxidation to CO_2 was essentially obtained together with formation of carbon deposits on the surface, which is responsible for catalyst deactivation.

The occurrence of oxidative dehydrogenation of cyclohexane to cyclohexene and benzene on MoO_3 or Mo/γ-Al_2O_3 catalysts in the temperature range 553–690 K has been reported [19]. Selectivity to dehydrogenated products is influenced by side-reactions such as combustion or cracking, leading to a heavy selectivity decrease at increasing temperature. A recent paper investigated the high temperature production of benzene from cyclohexane in vapor phase over several catalysts, such as V_2O_5/SiO_2, V_2O_5–Nb_2O_5/SiO_2, Ce-, V-, Fe-phosphates, H-ZSM5, Co-ZSM5 [20]. It was found that gas-phase reaction occurs above 850 K and selectivity to benzene is positively influenced by the presence of water vapor.

Very recently we found that cyclohexane is selectively oxidised to benzene on MoO_x/TiO_2 catalyst in the presence of gaseous oxygen at temperature of 308 K under UV illumination [21].

With the aim to confirm our preliminarily results [21], in this work we have extended the investigation by changing the molybdenum loading and nature of the support. The photocatalytic activity and selectivity of MoO_x supported catalysts on TiO_2, α- and γ-Al_2O_3 have been determined with a continuous flow gas–solid reactor.

2. Experimental

2.1. Catalysts preparation

All chemicals used in the experiments were HPLC grade obtained from Aldrich Co. TiO_2 as anatase phase, 80 m^2/g specific surface area containing 2 wt.% sulphate (DT51, Rhone Poulenc), α-Al_2O_3, 10 m^2/g (Aldrich) and γ-Al_2O_3, 144 m^2/g (Puralox SBA 150, SASOL S.p.A.) were impregnated with an aqueous solution of ammonium heptamolybdate $(NH_4)_6Mo_7O_{24}{\cdot}4H_2O$. Typical conditions were: 30 g of support, 2.5 l of solution, ammonium heptamolybdate concentration ranging between 2.4×10^{-4} and 1.0×10^{-3} M.

Powder samples were dried at 393 K for 12 h and calcined in air at 673 K for 3 h.

2.2. Catalytic tests

Fig. 1 reports a schematic picture of the experimental set up. Oxygen and nitrogen were fed from cylinders, nitrogen being the carrier gas for cyclohexane (CH) vaporised from a temperature controlled saturator. The gas flow rates were measured and controlled by mass flow controllers (Brooks Instrument). The reactor inlet or outlet gas were fed to an on-line quadrupole mass detector (MD800, ThermoFinnigan) and a continuous CO–CO_2 NDIR analyser (Uras 10, Hartmann & Braun).

The annular section of the photocatalytic reactor was realised with two axially mounted 500 mm long quartz tubes of 140 and 40 mm diameter, respectively. The reactor was

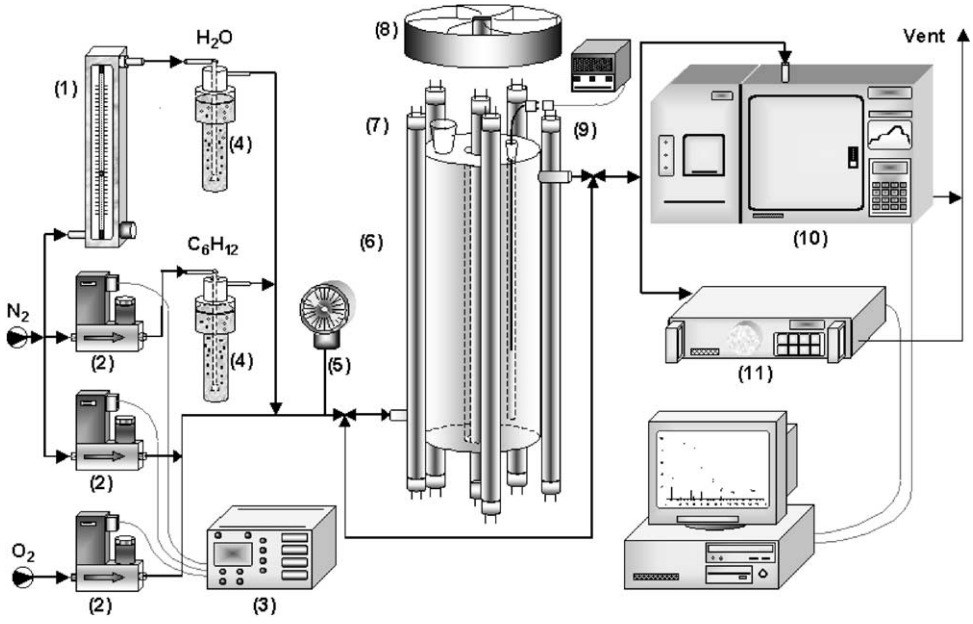

Fig. 1. Experimental set up apparatus: (1) rotameter; (2) mass flow controllers; (3) MFC control unit; (4) cyclohexane and water saturators; (5) manometer; (6) annular photoreactor; (7) UV lamps; (8) cooling system; (9) thermocouple; (10) GC-MS; (11) CO–CO_2 analyser.

equipped with seven 40 W UV fluorescent lamps providing photons wavelengths in the range from 300 to 425 nm, with primary peak centered at 365 nm. One lamp (UVA Cleo Performance 40 W, Philips) was centered inside the inner tube while the others (R-UVA TLK 40 W/10R flood lamp, Philips) were located symmetrically around the reactor. Both photoreactor and lamps were covered with reflectant aluminum foils. In order to avoid temperature gradients in the reactor caused by irradiation, the temperature was controlled to 308 ± 2 K by cooling fans.

The catalytic reactor bed was prepared in situ, by coating quartz flakes previously loaded in the annular section of a quartz continuous flow reactor with an aqueous slurry of catalysts powder. The coated flakes were dried at 393 K for 24 h in order to remove the excess of physisorbed water. This treatment resulted in uniform coating well adhering to the quartz flakes surface. The amount of deposited catalyst, evaluated by weighing the reactor before and after the coating treatment was 20 g. Catalytic tests were carried out feeding 830 Ncc/min N_2 stream containing 1000 ppm cyclohexane, 1500 ppm oxygen and adding 1600 ppm water to minimise catalyst photodeactivation [18].

The catalytic performance was evaluated as:

$$\text{CH}\,\%\,\text{conversion} = 100 \times \frac{\text{moles of inlet CH} - \text{moles of outlet CH}}{\text{moles of inlet CH}}$$

$$\text{BE}\,\%\,\text{selectivity} = 100 \times \frac{\text{moles of outlet BE}}{\text{moles of inlet CH} - \text{moles of outlet CH}}$$

$$\text{CO}_2\,\%\,\text{selectivity} = 100 \times \frac{\text{moles of outlet CO}_2}{6(\text{moles of inlet CH} - \text{moles of outlet CH})}$$

where CH is for cyclohexane and BE for benzene.

Total carbon mass balance was evaluated by comparing the inlet carbon as cyclohexane and the outlet carbon as the sum of unconverted cyclohexane and outlet benzene, cyclohexene, carbon mono- and dioxide.

2.3. Catalyst characterisation

Physico-chemical characterisation of catalysts was performed by different techniques. Surface area and porosity characteristics were obtained by N_2 adsorption–desorption isotherm at 77 K with a Costech Sorptometer 1040. Powder samples were treated at 423 K for 2 h in He flow (99.9990%) before testing. Laser Raman spectra of powder samples were obtained with a Dispersive MicroRaman (Invia, Renishaw), equipped with 785 nm diode-laser, in the range 100–2500 cm^{-1} Raman shift.

Chemical analysis was performed by inductive coupled plasma-mass spectrometry (7500c ICP-MS, Agilent) after microwave digestion (Ethos Plus from Milestone) of TiO_2-based samples in HNO_3/HCl and HF/HCl or of Al_2O_3-based catalysts in H_3PO_4/HNO_3 mixtures.

FTIR spectra of 1 wt.% catalyst in KBr disk were obtained with a Bruker IF 66 spectrophotometer in the range 4000–400 cm^{-1} (2 cm^{-1} resolution).

Temperature programmed desorption (TPD) experiment of catalysts after activity measurements were carried out at atmospheric pressure in a quartz flow reactor, connected on-line with CO, CO_2 (Uras 10E Hartmann & Braun) and with on-line quadrupole mass detector (MD800, ThermoFinnigan) in the range 293–773 K, with an heating rate of 10 K/min.

3. Results and discussion

The list of samples with nominal metal loading, surface areas, and main Mo-related bands from FTIR and Raman spectra are reported in Table 1. MoO_x coverage, calculated from the analysed MoO_3 loading and assuming a monolayer capacity of 0.12% (w/w) for MoO_3/m^2 [22,23], is 57% for 4MoDT and 100% for 8MoDT. A coverage degree of 42% was calculated for 8Moγ–Al, considering 18% Mo loading as the upper limit for monolayer formation, as estimated by Inamura et al. [24]. 108% coverage was obtained for 2Moα–Al [24].

A typical trend of photocatalytic test is reported in Fig. 2 with reference to 4MoDT. At the run starting time the nitrogen stream containing 1000 ppm cyclohexane, 1500 oxygen and 1600 water was passed through the reactor in the absence of irradiation at ambient temperature. Dark adsorption of cyclohexane was observed. Cyclohexane breakthrough time was about 10 min. Thereafter cyclohexane outlet concentration slowly increased to reach the inlet value after about 50 min, indicating that adsorption equilibrium of cyclohexane on the catalyst surface was attained. At that time the lamps were switched on: the cyclohexane outlet concentration immediately decreased to about 22% of the inlet value and then progressively increased with run time, reaching a steady state value corresponding to about 6% cyclohexane conversion after about 110 min. In the same figure the change of oxygen outlet concentration is also reported showing a general trend similar to that of cyclohexane. The analysis of products in the outlet stream disclosed the presence of benzene and (much lower amount) cyclohexene, as identified from the characteristic fragments m/z = 78, 77, 76, 74, 63, 52, 51, 50 (fragment 78 reported in Fig. 2) and 82, 67, 54, respectively (fragment 67 reported in Fig. 2), and of carbon mono- and dioxide, as detected by the NDIR analyser (Fig. 2).

It is worthwhile to note that both breakthrough time of the products and change of concentration with time are different for the different products. Fig. 2 shows that carbon dioxide is formed immediately after lamp switch on and reaches a maximum concentration value in about 30 min, slowly decreasing during the remaining run time. A parallel trend is

Table 1
List of catalysts and their characteristics

Catalysts	Nominal MoO_3 content (wt.%)	MoO_3 by ICP analysis (wt.%)	Specific surface area, BET (m^2/g)	Mo=O stretching[a], FTIR (Raman) (cm^{-1})
DT	0		71	–
4MoDT	4.7	4.4	68	957 (958, 970)
8MoDT	8.0	7.6	63	963 (956, 966, 978, 984, 995)
αAl	0		10	–
2Moα–Al	2.0	2.2	10	n.d. (925, 955, 980)
γAl	0		144	–
8Moγ–Al	8.0	7.6	147	n.d. (920, 949, 980)

n.d.: not determinable.
[a] In the range 900–1020 cm^{-1}.

shown by carbon monoxide concentration, but the values are one order of magnitude lower with respect to carbon dioxide. Instead, the outlet concentration of benzene progressively increases reaching a maximum value at greater time with respect to carbon dioxide. Then it decreases to a steady state value reached after about 220 min. A similar trend is shown by cyclohexene concentration, however the values are very much lower with respect to benzene.

In order to verify that cyclohexane was converted in a heterogeneous photocatalytic process, blank experiments were performed. A control test was carried out with the reactor loaded with uncoated quartz flakes. No conversion of cyclohexane was detected during this test, indicating the necessity of the catalyst for the observed reaction. A second test was performed with the catalyst loaded reactor, but switching the lamps off even after cyclohexane adsorption equilibrium was reached. In these conditions the composition of the outlet reactor was identical to that of the reactor inlet, indicating that no reaction occurred in dark conditions.

These results confirm the occurrence of photocatalysed cyclohexane oxydehydrogenation to cyclohexene and benzene together with deep oxidation to carbon oxides. Unexpected high selectivity to benzene is to be underlined.

The comparison of cyclohexane conversion on titania DT, 4MoDT and 8MoDT is shown in Fig. 3. On all catalysts a maximum value was reached after about 5 min, then activity decreased approaching a steady state conversion. On DT maximum cyclohexane conversion was about 25%, decreasing to 3% in 0.5 h. On 4MoDT the initial maximum of conversion was lower, about 21% after 8 min of illumination, but decreased less quickly with respect to DT: it is about 7% after 30 min and 6% after 2 h. Increasing Mo loading to 7.6 wt.% MoO_3 the initial maximum conversion was lower, about 15%, while steady state conversion was 2.3% after 0.5 h. Therefore the progressive coverage of titania surface by MoO_x species results in decreased initial cyclohexane conversion, while after illumination time of 110 min the conversion value on 4MoDT is about two times greater than on DT and 8MoDT.

While on DT the only reaction product is CO_2, both MoO_x/TiO_2 catalysts exhibit unexpected high selectivity to benzene. On 4MoDT (Fig. 4) maximum selectivity to benzene reached 31%, while maximum selectivity to carbon dioxide was 8%. On 8MoDT (Fig. 4) higher selectivity to benzene was observed (65% after 40 min) and maximum selectivity to carbon dioxide was 5%. With both catalysts the

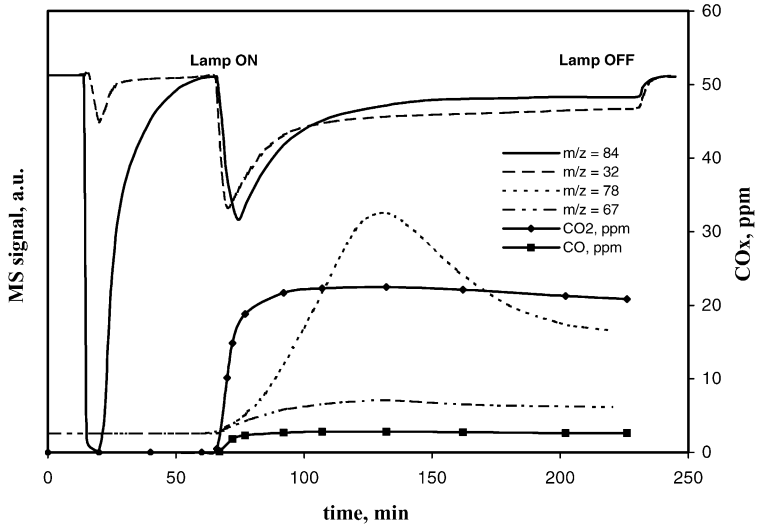

Fig. 2. Outlet reactor concentration (a.u.) of cyclohexane, oxygen and benzene and (ppm) of carbon mono- and dioxide as a function of run time. Feeding gas (830 Ncc/min): nitrogen containing 1000 ppm cyclohexane, 1500 ppm oxygen and 1600 ppm water. Weight of 4MoDT 20 g, reaction temperature 308 K.

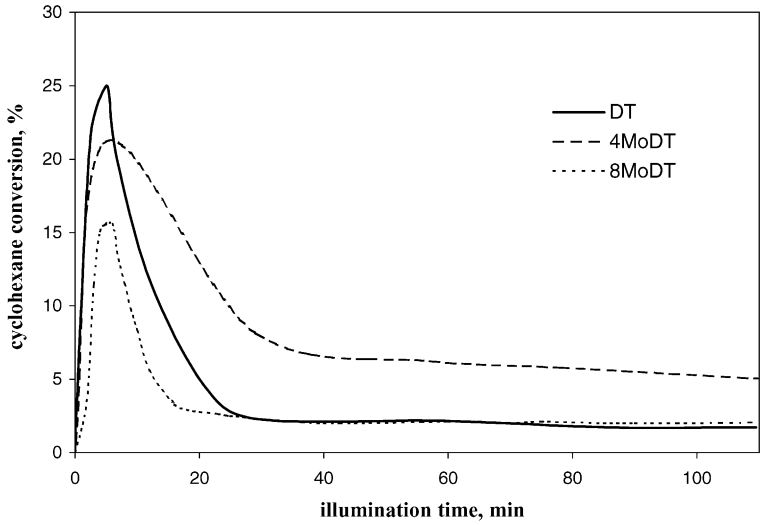

Fig. 3. Cyclohexane apparent conversion on MoDTs as a function of illumination time. Experimental conditions of Fig. 1.

presence of very low amounts of cyclohexene in the reaction products was detected (selectivity was about 0.7% on 4MoDT and 1.5% on 8MoDT). Therefore, the presence of MoO_x species on the surface of titania change the selectivity of the catalyst as more as higher is the molybdenum content.

In order to give better evidences of the effect of molybdenum oxide and titanium oxide in the observed selective oxidation of cyclohexane, catalytic tests were performed with 8Moγ–Al and 2Moα–Al. While both alumina supports did not exhibit any photoactivity, very low cyclohexane conversion, about 0.25%, was obtained on both catalysts, but the selectivity to CO_2 was close to 100%. Only few ppm of cyclohexene were detected in the first two minutes of reaction. Formation of benzene was not observed.

Therefore the catalytic results suggest that both titania and molybdenum oxide are essential in order to induce catalyst selectivity. Catalyst characterisation supports this conclusion.

FTIR spectra of TiO_2 supported catalysts showed Mo-related bands overimposed to typical absorptions from the support. For all Mo catalysts no MoO_3 crystallites sharp bands (Mo=O stretching vibrations at 992 cm^{-1} and bulk vibrations and 820 cm^{-1}) are present [25]. A band at 957 cm^{-1} on 4MoDT and at 963 cm^{-1} on 8MoDT is observed. The bands near 960 cm^{-1} can be assigned to the stretching mode of molybdenyl species in hydrated form [22,25,26]. In particular, they have been assigned to terminal Mo=O stretching of octahedral polymeric surface species [25]. For Mo-supported on α- and γ-alumina, clear bands of Mo species could not be obtained by FTIR transmission mode due to the strong absorption of the alumina support, as also reported by Inamura et al. [24].

Better evidence for Mo surface species was obtained by Raman spectra. On 2Moα–Al and 8Moγ–Al the main Mo=O band is, respectively, at 955 and 949 cm^{-1}. Other bands are present as shoulders at 920–925 and 980 cm^{-1}. On Mo–alumina catalysts Mo=O bands near 950 cm^{-1} are characteristic of Mo=O stretching mode of polymolybdenyl species [27]. Raman spectra of MoO_x/TiO_2 catalysts show a main band at 958 cm^{-1} on 4MoDT with a weak shoulder at

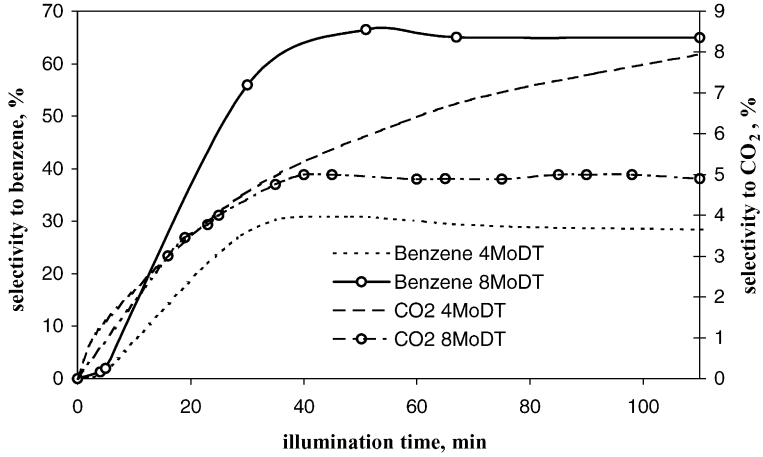

Fig. 4. Selectivity to benzene and CO_2 on MoDTs as a function of illumination time. Experimental conditions of Fig. 1.

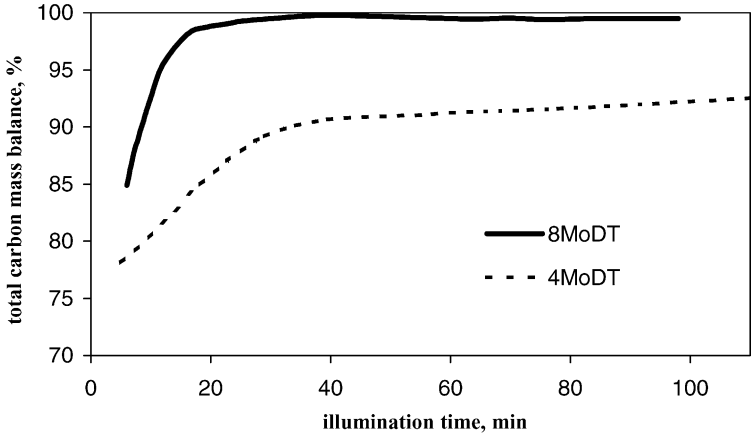

Fig. 5. Carbon and oxygen mass balance as a function of illumination time. Experimental conditions of Fig. 2.

970 cm^{-1}. On 8MoDT a complex band is observed due to the overlapping of 956, 966, 978, 984 and 995 cm^{-1} peaks. The increasing in wavenumbers with increasing Mo loading has been attributed to higher polymerisation degree of Mo species [28]. The small peak at 995 cm^{-1} indicates the incipient formation of segregated MoO_3 crystallites. Therefore, the surface is mostly covered by polymeric octahedrally anchored species for both MoDT catalysts. Nevertheless only titania supported catalyst are selective for the oxidation of cyclohexane, indicating that the interaction between titania and supported molybdenum oxide plays an essential role in changing the catalyst selectivity. The degree of interaction between molybdenum and the support can also be a reason for explaining the higher performances of titania supported catalysts. Moreover, Fig. 4 clearly shows the different shape of selectivity curves relevant to benzene and carbon dioxide, respectively. Carbon dioxide is likely formed immediately after lamp switch on mostly on titania sites, while benzene formation seems to require the formation of intermediate surface species, whose generation should be related to some interaction between support and molybdenum oxide surface species.

The examination of Figs. 3 and 4 shows that the activity of MoDT catalysts decreased during the time of illumination approaching an apparent steady state level in a couple of hours. A literature summary of catalyst deactivation in gas–solid photocatalysis was reported by Sauer and Ollis [29]. They showed that deactivation is a very commonly observed phenomenon, especially for single pass flow reactor, and concluded that its rationalisation requires further studies. However, catalyst deactivation should be likely related to adsorption/desorption of reactants and/or products of reaction.

Carbon mass balance evaluated as function of illumination time during the catalytic tests on 4MoDT and 8MoDT catalysts has been reported in Fig. 5. The carbon mass balance is close to 100% on 8MoDT and 90% on 4MoDT in steady state conditions. A significant fraction of inlet cyclohexane remained on the 4MoDT catalyst surface, as adsorbed cyclohexane and/or as converted cyclohexane to strongly adsorbed products.

TPD coupled with mass spectrometer and CO, CO_2 continuous analysers, in nitrogen flow, of 4MoDT catalyst after activity measurement in the range 293–773 K was performed. Desorption of cyclohexene ($m/z = 67$) from 373 up to 483 K, of benzene ($m/z = 78$) from 433 to 533 K, and of CO and CO_2 from about 423 up to 773 K were observed. No others products were found. Therefore, part of products remain adsorbed on the surface and could be related to the observed deactivation. It must be also noted that our deactivated samples do not appear brownished, as found by Einaga et al. [18]. They individuated carbon deposits on TiO_2 surface in heterogeneous photocatalytic decomposition of benzene, toluene, cyclohexane and cyclohexene, finding that deactivated TiO_2 catalysts were photochemically regenerated in the presence of water vapor and the carbon deposits were decomposed to CO_x.

Therefore preliminary characterisation of deactivated catalysts does not give any evidence for carbon deposit formation. Deeper investigation of this aspect is in progress.

4. Conclusions

The occurrence of photocatalysed heterogeneous oxidative dehydrogenation of cyclohexane in mild conditions, with high selectivity to benzene, has been observed on Mo-supported titania. Increasing molybdenum loading results in higher benzene selectivity, whereas titania alone is 100% selective to carbon dioxide. The selective formation of benzene is likely due to the presence of polymolybdate species supported on the titania surface. Nevertheless such species, when supported on α- or γ-alumina give very low activity and 100% selectivity to carbon dioxide. Therefore the role of titania is essential to obtain oxidative dehydrogenation products, likely due to its specific properties of photocatalyst. It could be argued that polymolybdate

species poison unselective sites of titania surface which would lead to total oxidation of cyclohexane.

Acknowledgment

The work has been funded by the Research National Council of Italy (CNR) through the project: Novel technologies for the synthesis of chemicals intermediates. Contract 98.03730.PF28.

References

[1] M. Anpo, Protecting the Environment, BHR Group, 1998.
[2] J.-M. Herrmann, Catal. Today 53 (1999) 115.
[3] A. Walker, M. Formenti, J.P. Meriaudeau, S.J. Teichner, J. Catal. 50 (1977) 237.
[4] N. Djeghri, S.J. Teichner, J. Catal. 62 (1980) 99.
[5] R.I. Bickley, G. Munuera, F.S. Stone, J. Catal. 31 (1973) 398.
[6] M. Formenti, J.P. Meriaudeau, S.J. Teichner, CHEMTECH 1 (1971) 680.
[7] K. Wada, K. Yoshida, Y. Watanabe, T. Suzuki, Appl. Catal. 74 (1991) 1.
[8] M.L. Sauer, D.F. Ollis, J. Catal. 158 (1996) 570.
[9] D.S. Muggli, J.L. Falconer, J. Catal. 175 (1998) 213.
[10] A. Maldotti, R. Amadelli, G. Varani, S. Tollari, F. Porta, Inorg. Chem. 33 (1994) 2968.
[11] A. Maldotti, R. Amadelli, V. Carassiti, A. Molinari, Inorg. Chim. Acta 256 (1997) 309.
[12] A. Molinari, A. Maldotti, R. Amadelli, A. Sgobino, V. Carassiti, Inorg. Chim. Acta 272 (1998) 197.
[13] C. Giannotti, C. Richter, Int. J. Photoenergy 1 (1999) 1.
[14] K. Teramura, T. Tanaka, T. Yamamoto, T. Funabiki, J. Mol. Catal. A: Chem. 165 (2001) 299.
[15] C.B. Almquist, P. Biswas, Appl. Catal. A 214 (2001) 259.
[16] F. Blatter, H. Sun, S. Vasenkov, H. Frei, Catal. Today 41 (1998) 297.
[17] F. Blatter, H. Frei, J. Am. Chem. Soc. 118 (1996) 6873.
[18] H. Einaga, S. Futamura, T. Ibusuki, Appl. Catal. B: Environ. 38 (2002) 215.
[19] E.C. Alyea, M.A. Keane, J. Catal. (1996) 28.
[20] M. Panizza, C. Resini, G. Busca, E.F. Lòpez, V.S. Escribano, Catal. Lett. 89 (2003) L-4.
[21] P. Ciambelli, G. Lisanti, D. Sannino, V. Palma, The TPCAT 4 Pre-Conference Symposium in Kobe – Catalysis for the Environment and New Energy Sources, Kobe, Japan, July 12, 2002.
[22] K.Y.S. Ng, E. Gulari, J. Catal. 92 (1985) 340.
[23] D.S. Kim, Y. Kurusu, I.E. Wachs, F.D. Hardcastle, K. Segawa, J. Catal. 120 (1989) 325.
[24] S. Inamura, H. Sasaki, M. Shono, H. Kani, J. Catal. 177 (1998) 72.
[25] H. Matralis, S. Theret, Ph. Sebastians, M. Ruwet, P. Grange, Appl. Catal. B 5 (1995) 271.
[26] L. Lietti, P. Forzatti, L.J. Alemany, G. Busca, E. Giamello, F. Bregani, Catal. Today 29 (1996) 143.
[27] I.E. Wachs, Catal. Today 27 (1996) 437.
[28] C.P. Cheng, G.L. Schrader, J. Catal. 60 (1979) 276.
[29] M.L. Sauer, D.F. Ollis, J. Catal. 163 (1996) 215.